

X-RAY IMAGE PROCESSING OF BONE CAVITY FILLED WITH BIOMATERIALS BASED ON PHOSPHATE CALCIUM

SALMA HAKIM^{1,2}, ABDELAZIZ ESSAKHI^{1,2,3}, , MANAL EZZAHMOULY^{1,2} ABDELKADER BOULEZHAR³, ABDELMAJID ELMOUTAOUAKKIL¹, ZINEB HATIM²

¹ Research Laboratory in Optimization, Emerging Systems, Networks and Imaging, LAROSERI, Computer science Department, Chouaïb Doukkali University, El Jadida, Morocco

² Energy, Materials and environment Team, Chemistry Department, Chouaïb Doukkali University, El Jadida, Morocco

³ Laboratory of Renewable Energie and System Dynamics (LERDYS) Faculty of Sciences Ain Chock, Casablanca Maroc.

E-mail : hakim.s@ucd.ac.ma, Essakhi aziz@yahoo.fr, ezzahmoulymnl@gmail.com
boulezhara@gmail.com , zineb.hatim@yahoo.fr, elmsn@hotmail.fr

ABSTRACT

Certain traumatic situations, congenital diseases or cancers can cause bone loss and require bone grafts or implants. Bone substitutes prepared from calcium phosphates such as hydroxyapatite ($\text{Ca}_{10}(\text{PO}_4)_6(\text{OH})_2$) or Beta-tricalcium phosphate ($\beta\text{-Ca}_3(\text{PO}_4)_2$) are used in orthopedic and dental surgery and they present good biocompatibility and bioactivity. These biomaterials in different forms: paste, granule or screw and their biological integration is influenced by structure and microstructure as well as the architecture, porosity, location and bone / implant connectivity. The aim of this study is segmenting and analyzing nano-biocomposite granules with low crystalline structure from bone. The simple thresholding is not sufficient, for that we have developed a novel method that combine different segmentation methods and then determine the volume of the defect, segmented the granules in the defect, calculate their size distribution.

Keywords: *Image Processing, X-Ray Tomography, Segmentation, Bio-Materials, Calcium Phosphate Granules, Bone Filling*

1. INTRODUCTION

Calcium phosphate biomaterials have been used worldwide for more than 20 years as bone replacement materials and have become the most implanted bioactive materials, especially in orthopaedic and dental surgery. These compounds can bind chemically in skeletal tissue, including planting calcium phosphate on the surface of the tissue from biological fluids [1]. The biomaterials used to treat bone tissue are hydroxyapatite ($\text{Ca}_{10}(\text{PO}_4)_6(\text{OH})_2$: HA), tricalcium phosphate ($\beta\text{-Ca}_3(\text{PO}_4)_2$): $\beta\text{-TCP}$ and biphasic HA/ $\beta\text{-TCP}$ mixture. These biomaterials have good biocompatibility and bioactivity and their chemical composition is similar to that of human ash [2]. These biomaterials have good biocompatibility and biocompatibility due to their chemical composition, as well as the biocompatibility and biocompatibility of human skeletal apatite.

The use of calcium phosphate biomaterials in various forms as frames or pastes with a highly crystallized structure has significantly increased therapeutic performance to allow bioactive alternatives to fully adapt to defects remaining skeletal [3]. However, this form of alternative is very intensive, which means that it is not sufficiently absorbed. Biomaterials are also used in granulated form to fill in small skeletal defects (typically 0.1 to 5 mm in diameter). The particles occupy the space of the skeleton and create macroporosity allowing invasion of bone cells [4]. Because of its importance for clinical and scientific applications, imaging is now considered an important tool for bone processing. The most popular imaging methods in medicine include X-rays, MRI, and ultrasound and computed tomography. These methods are often very cost-effective, efficient and easy to use [5]. In this case, X-rays are considered the most appropriate tool for

implant adaptation. Computer-aided tomography (CT-scan), a 3D bone analysis method, is the most widely used method, as it is the fastest and easiest way for doctors to study bone and joint damage. Physicians generally use X-rays to determine the presence of a defect and the location of the implant. The database is a DICOM image. Modern hospitals store medical images in standard DICOM format (digital review and medical communication), including text in the image. Any attempt to retrieve and display these images must go through PACS (Picture Archives and Communication System) hardware. Usually, the biomaterials filled in the defect bone could be confused with the bone because they have similar level grey, for that the use of an automatic segmentation method that detects the biomaterials and separate it from the bone.

The rest of the paper is organized as follows:

- The second section present the state of the art
- The third section present materials used in the work and our proposed method
- The fourth section present results obtained from our method and we discuss this results
- The final section present the conclusion and perspectives

2. EARLIER WORK

Baptiste Arbez et al [6] presented a paper on the qualitative and quantitative evaluation of the three-dimensional microstructure of several granular biomaterials manufactured and marketed by several companies, comparing their properties to those of human bone trabecular and verifying the molecular composition of these biomaterials by Raman microspectroscopy. Homologous and heterologous particles as well as synthetic Ca/P ceramic particles commonly used in maxillofacial surgery were studied. The effects of the two particle sizes proposed by the industry (250-1000 μm and 1000-2000 μm) on the three-dimensional microstructure were also studied.

Vijaykumar V et al [7] presented an algorithm for filtering the Gaussian noise, then replace the center pixel by the mean of the sum of the surrounding pixels based on a threshold value.

Generally the DICOM images are corrupted by the salt and pepper noise.

Tomazevic et al [8] proposed a manual and semi-automatic method for interactive segmentation of bone tissue. They used a threshold-based segmentation method to detect bone tissue in CT images.

Al-Khaffaf H et al [9], proposed an extension of the K-fill algorithm to remove salt and pepper noise based on the number of black or white pixels in a 3×3 window Assuming that the image is contaminated by noise, which is modeled as the sum of two random processes: Poisson and Gaussian, this method jointly estimates the scale parameter of the Poisson component and the mean and variance of the Gaussian component.

In their work, Xiaoli Zhang et al [10] proposed a new thresholding algorithm based on Otsu 3D and multi-scale image representation. The whole segmentation algorithm is designed as an iterative process. In each iteration, the image is segmented using an efficient 3D Otsu, and then fast local Laplace filtering is used to obtain a smooth image that is fed into the next iteration. Finally, the segmentation results are combined and the final segmentation result is obtained by majority vote.

Sweedy et al [11] presented a segmentation method to isolate the three phases present in the explanted ceramic bone substitute scaffolds, i.e. bone, ceramic remnants, and soft tissue. For that purpose, a contour-based method combined with a compaction algorithm specifically treating the fuzzy grey-intensity transitions often found between phases were used to yield more accurate results than those of currently existing global thresholding methods. Then aligning pre- and post-implantation micro CT datasets, hence allowing the extraction of the grey intensity value distribution of each phase.

M.C. Jobin Christ et al [12] proposed a methodology that combine KMeans clustering with marker marker controlled watershed segmentation algorithm and also combine Fuzzy CMeans clustering with marker controlled watershed segmentation algorithm separately for medical image segmentation.

Anu T C, Mallikarjunaswamy M.S et al [13] developed an image processing based on

preprocessing segmentation, edge detection and feature extraction methods. The processed images are further classified into the fractured and non-fractured bone.

Javier Cardona et al [14] proposed in their study an image analysis framework that combines standard image processing steps, as median filter in order to remove noise and laplacian for edge detection, object closing and filling, removal of object on frame boundary and filtering the objects of small sizes, with an additional focus evaluation.

Ezzahmouly et al [15] presented a method based on mathematical morphological operations, to determine the microstructure, the morphological characteristics and classes of pores of the prepared hydroxyapatite bioceramic. It compute successive openings operation with structuring element increasing in diameter to close the holes progressively. The difference between the image before and after an opening corresponds to the total volume of the hole being closed.

Siyao shao et al [16] presented a hybrid bubble hologram processing approach for measuring the size and 3D distribution of bubbles over a wide range of size and shape. The proposed method consists of five major steps, including image enhancement, digital reconstruction, small bubble segmentation, large bubble/cluster. Segmentation, and post-processing.

In her paper, Samantha J. Polak [17] presents an automated micro computed tomography (microCT) image segmentation algorithm that segments bone, calcium phosphate (CaP) bone scaffolds, and soft tissue. The authors used micro tomography to characterize bone growth in CaP scaffolds in a large, non-destructive dataset, accurately and at high throughput (more than 100 samples). The method involves identifying soft tissue that resembles the background of the samples and using the Fournier transform to filter the images and determine the orientation of the scaffold rods in each image. Based on the orientation of the identified rods and the periodicity of the network, they were able to distinguish the scaffold from the bone in each image. Finally, the segmentation of the three materials was refined using stress edge detection.

3. MATERIALS AND METHODS

3.1 Biomaterials Fabrication

Work is carried out on bovine sponges generally containing mineral and organic phases. A first treatment consists in eliminating the organic part which poses a problem of conservation of the bones. Decreasing of the bones was carried out in solvent baths which are alcohols (C_2H_5OH), oxidants (H_2O_2) and bases (KOH).

The study used nano-biological composite particles of calcium phosphate. The biological material was obtained by the method described by Elouahli [18]. The polymer (chitosan)/nano-apatite is suspended in the gel bath with a syringe and dried at 37 degrees.

Figure 1 shows the spherical view of the particles, and the SEM image shows that the particles are about 10 nm in size. Compared to existing biomaterials Nanocrystalline biological composites must be prepared to improve biological properties. These particles have good size and structural stability and can be treated without damage.

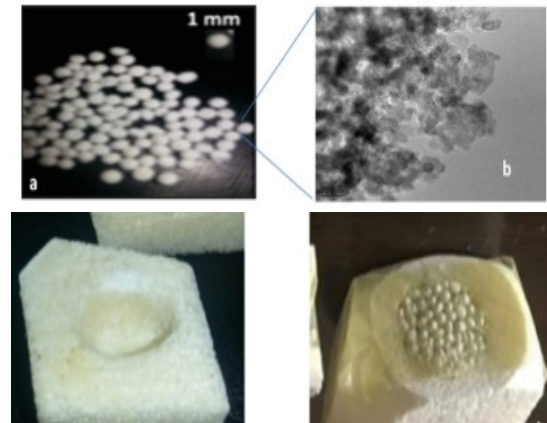


Figure 1: Photography of spongy bone with induced cavity and Photography of cavity with granules

3.2 X-Ray Scanning

Today, three-dimensional (3D) imaging is one of the successful clinical applications. It has many advantages compared to the two-dimensional (2D) X-ray imaging used as an important tool to accurately determine the structure of bone defects and correct the position of implants. [4], [19].

This imaging technique, generally used by the clinician to achieve successful implementation. Tomographic imaging consists of directing X-rays at an object from multiple orientations and measuring the decrease in intensity along a series of linear paths. This decrease is characterized by

Beer's Law, which describes intensity reduction as a function of X-ray energy, path length, and material linear attenuation coefficient.

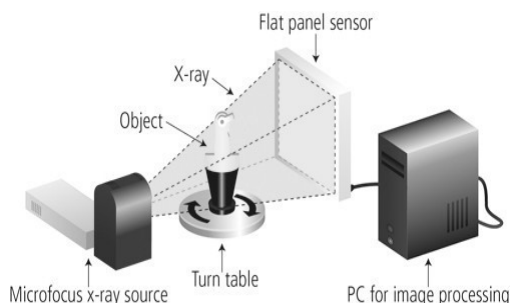


Figure 2: X-Ray Tomography Principles

Beer-Lambert's law thus relates the absorption of light to the material that passes through it. Similarly, the absorption of X-rays is related to the material through which the light beam passes, according to the following equation (Jackson & Hawkes, 1980)

$$I=I_0 \exp(-\mu t) \quad (1)$$

Where I = intensity of transmitted X-rays

- I_0 = intensity of incident X-rays
- μ = linear attenuation coefficient of the material
- t = thickness of material through which X-rays have traveled [20, 21]

A special algorithm is then used to reconstruct the distribution of X-ray attenuation in the image volume. Image reconstruction is the step where the digitized data set is processed to produce an image. The image is digitized and consists of a matrix of pixels. Filtered back-projection is an image processing algorithm used in computed tomography to create or "reconstruct" images. Figure 3 illustrates the principle of the image reconstruction process. The final step is the conversion of the digital image into a visible and viewable analog image (shades of gray) [22, 23].

Thus, tomography allows access to the core of the biomaterial and to study the microstructure of the implant and the bone-implant contact zone through the changes in X-ray absorption. This technique also allows to see the shape and volume

of the desired filling as well as the integration of the implant in the bone.

This study was carried out at IBN ROCHD hospital in Casablanca, using a sixteen-bar X-ray scanner correctly adjusted to provide a better resolution. The device used is third generation scanner; there is not a single detector, but several detectors in action during a rotation of the x-ray tube around the patient, this scanner takes less than 0.4 s to perform a round. The acquisition time of the image is fast and we obtain very high resolution imagery. [24]

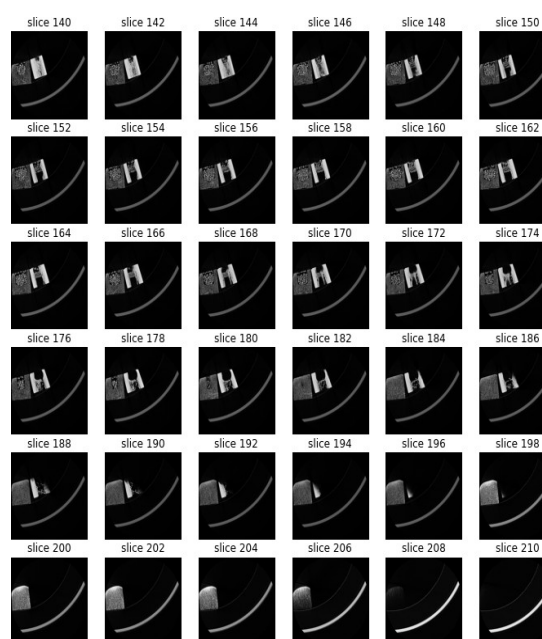


Figure 3: Slices of Bone Cavity Filled with Biomaterials Granules

3.3 Proposed Imaging Method

In order to calculate the number of granules filled in the induced defect and also the granular size we have first extract the biomaterials from bone, but it is difficult since biomaterial and bone have the same level gray. To surpass this problem we have used an adaptive method that combine several methods of segmentation. The method aims specially to separate biomaterial from bone.

First we proceed by the pre-processing step where we used the median filter, it is a non-linear digital filtering method used to eliminate salt and pepper noise. Then we classified the images using K-means in order to separate the bone from

the background. After that we segment the results using a combination of several methods as thresholding, erosion, and watershed. Finally, we save the new volume and calculate the different measurement as number of granules and their size.

In the first step, we apply the preprocessing. Noise can be defined as unwanted image pixels that affect image quality. We write $(x, y) = g(x, y) + n(x, y)$ where f is the noisy image, g is the original image and n is the noise present in the image. Different types of noise could be presented in the image such as Gaussian noise, Salt and pepper noise etc. The Salt and pepper is one of the noise mostly presented in x-ray images. This usually caused by detecting or transmitting errors that appear as light and black dots in the image. It can be removed by applying mathematical transformations on the images, preserving edges while suppressing noise. Median filter is a non-linear digital filtering method used to eliminate salt and pepper noise. [25]

To separate the foreground (bone filled) from the background (Air) we use K-Means method. Classification is a step in data analysis to examine the dataset and it classifies them into several categories. Each class has its own characteristics and the data that belong to such class have the same properties of this class. Many practical problems are easy to solve. K-Mean is best suited for biomedical image segmentation.

Steps of the K-Means algorithm:

- Choose k cluster centers to coincide with k randomly chosen patterns inside the hyper volume containing the pattern set. (C)
- Assign each pattern to the closest cluster center. ($C_i, i = 1, 2, \dots, C$)
- Recompute the cluster centers using the current cluster memberships. (U):

$$u_{ij} = \begin{cases} 1 & \text{if } \|x_j - c_i\|^2 \leq \|x_j - c_k\|^2 \\ 0 & \end{cases}$$

- for each $k \neq i$
- If a convergence criterion is not met, go to step 2 with new cluster centers by the following equation, i.e., minimal decrease in squared error:

$$c_i = \frac{1}{|G_i|} \sum_{k \in G_i} X_k$$

Where, G_i is the size of G_i

$$|G_i| = \sum_{j=1}^n u_{ij}$$

After that we calculate the mean of centers, then we apply threshold method which converts a gray-scale image into a binary image where the two levels are assigned to pixels that are below or above the calculated mean.

To erode away the finer element we proceed by the erosion operation which is a mathematical morphology. This is one of the two most important morphological operations (the other is dilation) and all other morphological operations are based on. Erosion operations generally use structural elements to recognize and reduce the shapes contained in the input image. It can be written as:

$$A \oplus B = \bigcup_{b \in B} A_b$$

In order to obtain the mask of biomaterials, we label in first the eroded image after that we choose the good labels we are interest in and then apply the dilation operation which usually uses a structuring element for probing and expanding the shapes contained in the input image and it can be written as:

$$A \ominus B = \{z \in E | B_z \subseteq A\}$$

After this process we obtain the final mask of biomaterials filled in the induced defect. Then we apply the mask on the original image, we threshold the result and we apply another erosion operation in order to eliminate unwanted pixels.

We repeat the whole process until the biomaterials are segmented definitely from the bone. Then we apply the watershed method in order to separate the connected granules from each other. Steps of the watershed algorithm are:

- A set of tags, pixels that start a flood, are selected.
- The adjacent pixels for each selected area are inserted into the priority queue and their priority level corresponds to the pixel gradient.

- Pixels with the highest priority are extracted from the priority queue. If the neighbor of the selected pixel has the same label, the pixel is marked as its label. All unidentified neighbors who are not yet in the priorityqueue are placed in the priority queue.
 - Repeat step 3 until the priority queue is empty.
- Finally, we save the new volume and calculate the size and distribution of these granules.

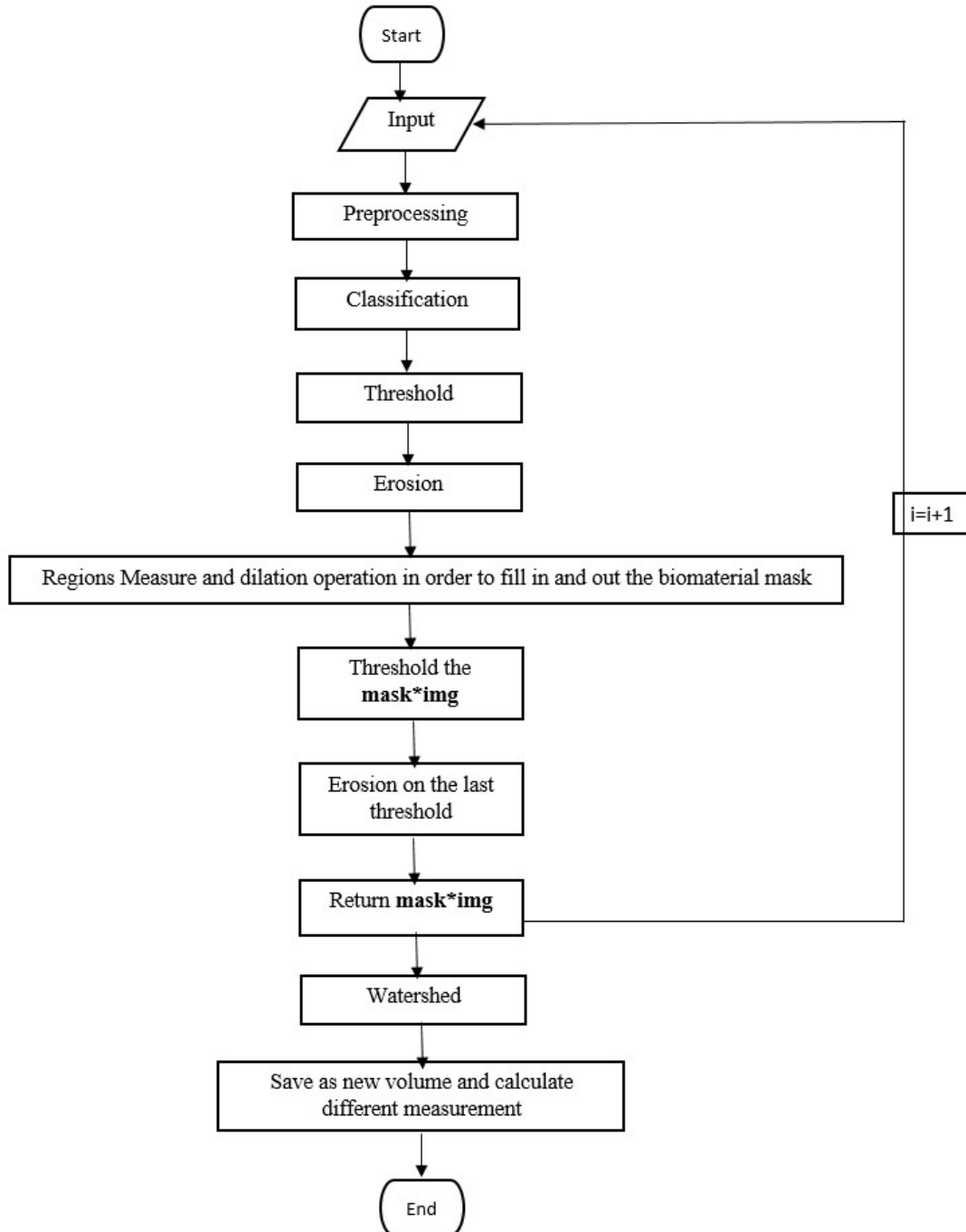


Figure 4: Flowchart of the method

4. RESULTS AND DISCUSSION

In this study, we used a spongy bone sample from bovine. The induced cavity was filled with a spherical particle consisting of a medium-sized nanobiological calcium phosphate.

We used radiography to describe and quantify the defective bone. The images have been analyzed using the method described in the previous section, which we have segmented the granules and calculate their size distribution.

The following figures present results of our proposed method, which we could visualize that biomaterials were separated from the bone and then we could calculate the hole volume and size of each granular. This study will help us to detect the biomaterials from the image in order to follow-up their regeneration in the in –vivo study.

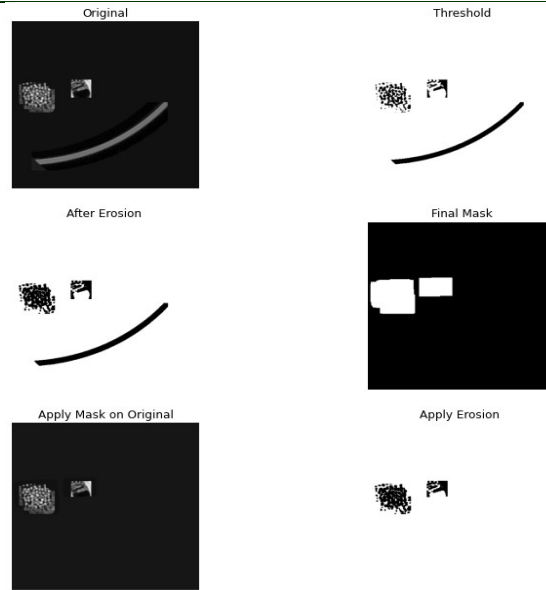


Figure 6: Segmentation of the Biomaterial from Bone (Second iteration)

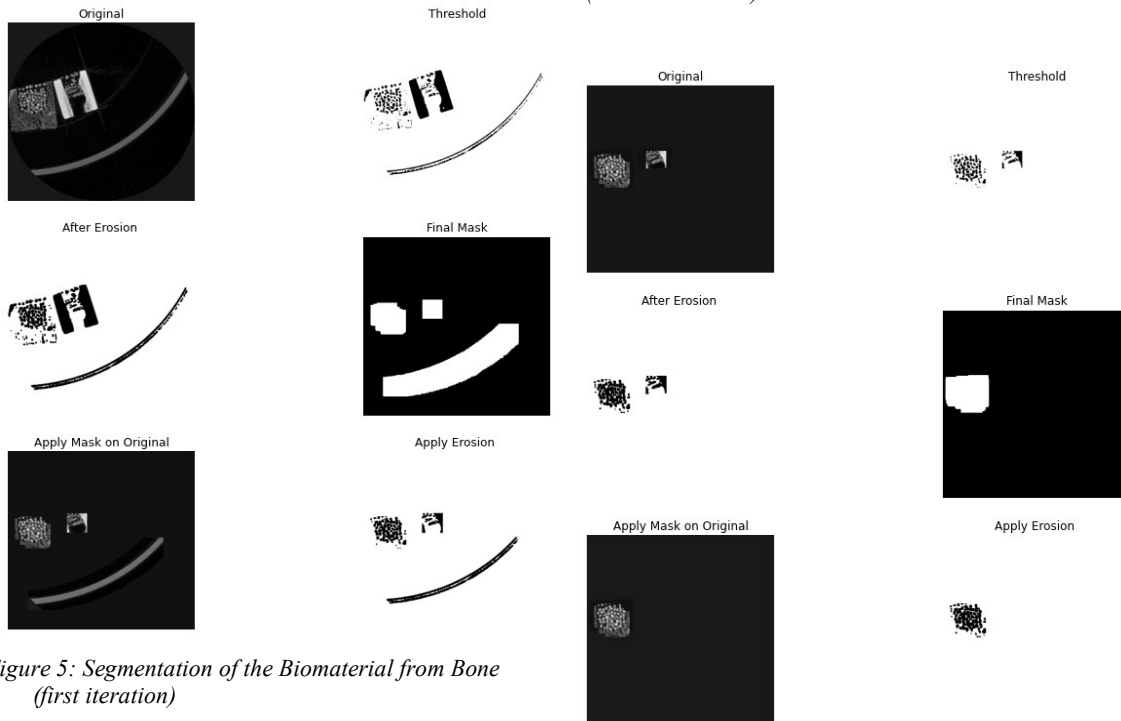


Figure 5: Segmentation of the Biomaterial from Bone (first iteration)

Figure 7: Segmentation of the Biomaterial from Bone (Third iteration)

Table 1 summarizes the results of the processing applied on scanner images of the unfilled bone. It allowed us to calculate the volume of the induced defect (373 mm³). We have been determined the distribution of number and size of granules in (Table 2).

Table 1: Size of the Induced Defect

Number of Pixel	Volume of Voxel (mm ³)	Volume of Hole (mm ³)
16954	0.022	373

Table 2 summarizes the results of our proposed method on images of bone defect filled with granules, the method allowed us first to calculate for each granular it size. We observe that number of granules between 0.8 and 1.0 mm is 300 and the number of granules between 1.0 and 1.6 is 22 and the number of granules between 1.6 and 2.1 is 39, these results show good compatibility with the real distribution.

Table 2: Granules Size Distribution

Granular Size (mm)	Number of Granules
Less than 0.8	0
0.8-1.0	300
1.0-1.6	22
1.6-2.1	39
Greater than 2.1	0

The results show that the calculated values of the defective bone volume and the extracted granules volume are very close. Thus, the proposed method allows accurate control of cavity filling. The automated method presented in this paper can be advantageously used in medical imaging, especially in the field of bone tissue engineering. It can be used to highlight the geometry of bone defects and to design and control prefabricated 3D structures. After surgery, the proposed method can also be used to monitor the integration of the implant and the regenerated bone.

The method offers the advantages of a thresholding method in terms of speed and simplicity, by first eliminating background noise and improving the contrast of tomographic images.

After applying the segmentation methods, we extract geometric information from the images.

To evaluate our method, the induced bone defect was filled by a biomaterial in the form of granules. Location of the implant in the bone defect has been evaluated using the x-ray scanner technique. The perfect integration of biomaterials into the defect has been observed. The proposed method allowed us to calculate different morphological parameters, segmented, isolate and extracted the implant and calculate its volume.

The distribution of particles shows a medium size centered between 0.8 and 1 mm. The image results are consistent with the real values, thus validating the chain of processing the images that have been used. The volume of the empty defect calculated by our method allows, in the clinical case, to prepare the filling determining the form and the volume before carrying out the filling process. The results obtained after filling determine the quality of filling and allow the follow-up of filling in in vivo cases.

5. CONCLUSION AND PERSPECTIVES

We analyzed the microstructure of calcium phosphate particles in a defective bone using a medical X-ray scanner and evaluated these images using our novel image processing method. The information obtained is useful for both patients and bio-material manufacturers. In fact, the image processing allows:

- Observe the shape of the bone cavity and the condition of its surroundings.
- Calculate the volume of cavities which need to be re-paired
- Predict the volume and the shape of the Bio-material before the filling act
- Evaluate the distribution of granules in the bone defect
- Follow-up of the integration and the evolution of the implant in the bone matrix.

As the perspective of this work, we aim to calculate the volume contact of granules and establish the relation between their size and the volume of the porosity. We are interested also to test other forms of biomaterials and follow, by scanner medical, the filling of the defect bone in vivo and the developing new image processing methods.

REFERENCES:

- [1] Combes, C., Rey, C.: Biomateriaux a base de phosphates de calcium. *Techniques de l'Ingenieur* 33, 1–19 (2013)
- [2] Dalmonico, G.M.L., Franczak, P.F., Levandowski Jr., N., Camargo, N.H.A., Dallabrida, A.L., da Costa, B.D., Canillas, M.: An in vivo study on bone formation behavior of microporous granular calcium phosphate. *Biomater. Sci.* 5(7), 1315–1325 (2017)
- [3] Janvier, P., Verron, E.: Ciments pour le comblement de defect osseux. *Techniques de l'ingenieur Materiaux pour la sant'e et l'agroalimentaire* (2014)
- [4] Arbez, B., Kun-Darbois, J.D., Convert, T., Guillaume, B., Mercier, P., Hubert, L., Chappard, D.: Biomaterial granules used for filling bone defects constitute 3D scaffolds: porosity, microarchitecture and molecular composition analyzed by microCT and Raman microspectroscopy. *J. Biomed. Mater. Res. Part B: Appl. Biomater.* 107(2), 415–423 (2019)
- [5] Shubhangi, D.C., Raghavendra, S., Hiremath, P.S.: Edge detection of femur bones in X-ray images, a comparative study of edge detectors. *Int. J. Comput. Appl.* 42(2), 13–16 (2012)
- [6] Arbez, Baptiste, et al. "Biomaterial granules used for filling bone defects constitute 3D scaffolds: porosity, microarchitecture and molecular composition analyzed by microCT and Raman microspectroscopy." *Journal of Biomedical Materials Research Part B: Applied Biomaterials* 107.2 (2019): 415-423
- [7] Vijaykumar, V., Vanathi, P., Kanagasabapathy, P. (2010). Fast and efficient algorithm to remove gaussian noise in digital images. *IAENG International Journal of Computer Science*, 37(1).
- [8] TOMAZEVIC, M., KREUH, D., KRISTAN, A., et al. Preoperative planning program tool in treatment of articular fractures: process of segmentation procedure. In : XII Mediterranean conference on medical and biological engineering and computing 2010. Springer, Berlin, Heidelberg, 2010. p. 430-433.
- [9] Al-Khaffaf, H., Talib, A. Z., Salam, R. A. (2008). Removing salt-and-pepper noise from binary images of engineering drawings. In: *Pattern Recognition. ICPR. 19th International Conference on*, p. 1–4. IEEE.
- [10] Feng, Yuncong, et al. "A multi-scale 3D Otsu thresholding algorithm for medical image segmentation." *Digital Signal Processing* 60 (2017): 186-199.
- [11] Sweedy, A., Bohner, M., van Lenthe, G. H., & Baroud, G. (2017). A novel method for segmenting and aligning the pre-and post-implantation scaffolds of resorbable calcium-phosphate bone substitutes. *Acta biomaterialia*, 54, 441-453.
- [12] Christ, M. J., & Parvathi, R. M. S. (2012). Medical Image Segmentation using Fuzzy C-means clustering and Marker Controlled Watershed algorithm. *International Journal of modern engineering research*, 2(1), 408-411.
- [13] Anu, T. C., & Raman, R. (2015). Detection of bone fracture using image processing methods. *Int J Comput Appl*, 975, 8887.
- [14] Cardona, J., Ferreira, C., McGinty, J., Hamilton, A., Agimelen, O. S., Cleary, A., ... & Tachtatzis, C. (2018). Image analysis framework with focus evaluation for in situ characterisation of particle size and shape attributes. *Chemical Engineering Science*, 191, 208-231.
- [15] Ezzahmouly, M., ElMoutaouakkil, A., Ed-dahraouy, M., Hakim, S., EL Byad, H., Gourri, E., Hatim, Z. Development of an Automatic Process for Calculation of Bone Defected Volume from Tomographic Images. Available at SSRN 3903254.
- [16] Shao, S., Li, C., & Hong, J. (2019). A hybrid image processing method for measuring 3D bubble distribution using digital inline holography. *Chemical Engineering Science*, 207, 929-941.
- [17] Polak, Samantha J., et al. "Automated segmentation of micro-CT images of bone formation in calcium phosphate scaffolds." *Computerized Medical Imaging and Graphics* 36.1 (2012): 54-65.
- [18] Elouahli, A.: Preparation et caracterisation de poudre pure de phosphate tricalcique. Application `a la mise au point d'un nouveau nano-composite phosphate tricalcique apatitique/chitosane pour usage orthopedique et dentaire. Thesis in Chemistry. Under direction of Z. Hatim. El Jadida. Chouaib Doukkali University (2017)
- [19] Hakim, S., Ezzahmouly, M., El Ouahli, A., El Haddaoui, S., Siwan, A., El Moutaouakkil, A., & Hatim, Z. (2019, July). Image Processing of X-Ray Images of Empty and Filled Bone Cavity by Calcium Phosphate Granules Using ImageJ. In *International Conference on Advanced*

- Intelligent Systems for Sustainable Development (pp. 206-212). Springer, Cham.
- [20] Nagarajan, Aishwarya, et al. "Diagnostic imaging for dental implant therapy." *Journal of clinical imaging science* 4.Suppl 2 (2014).
- [21] Kelkar, Shivangi, Carol J. Boushey, and Martin Okos. "A method to determine the density of foods using X-ray imaging." *Journal of food engineering* 159 (2015): 36-41.
- [22] Seeram, Euclid. "Computed tomography: physical principles and recent technical advances." *Journal of Medical Imaging and Radiation Sciences* 41.2 (2010): 87-109.
- [23] Willeminck, Martin J., and Peter B. Noël. "The evolution of image reconstruction for CT—from filtered back projection to artificial intelligence." *European radiology* 29.5 (2019): 2185-2195.
- [24] Pelé, C., Bujoli, B., Guilminot, É., Lemoine, G., Louvet, I., & Poisson, L. (2015). ANALYSIS OF FATTY ACIDS EXTRACTED FROM A WHALE SKELETON: ANALYTICAL APPROACH TO EVALUATE THE EFFICACY OF DEGREASING TREATMENT. *Journal of the American Institute for Conservation*, 54(3), 168-180.
- [25] Brownrigg, D. R. (1984). The weighted median filter. *Communications of ACM*, 27(8), 807-818